第37卷第7期 无 机 化 学 学 报 Vol.37 No.7
2021年7月 CHINESE JOURNAL OF INORGANIC CHEMISTRY 1277-1283

以DNA为靶点的钌(Ⅱ)配合物的合成、晶体结构和抗肿瘤活性

盖爽爽[1] 蓝峻峰[2] 张 鹏[1,2] 蒋才云*[,1,2] 覃逸明*[,1,2]
([1]广西科技师范学院,特色瑶药资源研究与开发校级重点实验室,来宾 545004)
([2]广西科技师范学院食品与生化工程学院,来宾 545004)

摘要: 为开发新型钌(Ru)抗肿瘤药物,以3-甲基-2-噻吩甲醛-4-羟基苯甲酰肼席夫碱配体(L)合成了[Ru(L)(DMSO)$_2$Cl$_2$] (**1**)(DMSO=二甲基亚砜)。用X射线单晶衍射法测定了**1**的晶体结构。配合物**1**的结构由1个Ru(Ⅱ)中心离子与2个DMSO分子、2个氯离子、1个L配位而成。通过MTT实验分析,**1**对T24细胞表现出良好的抗肿瘤活性。同时,通过彗星实验、蛋白质印迹实验和DNA琼脂糖凝胶电泳实验结果证明**1**可以有效结合DNA,诱导DNA损伤,最终杀死肿瘤细胞。导致DNA损伤的原因很可能是由于细胞与**1**孵育后细胞内可以产生大量的活性氧。

关键词: 钌(Ⅱ)配合物; DNA靶点; T24细胞; 抗肿瘤活性
中图分类号: O614.82$^+$1 **文献标识码:** A **文章编号:** 1001-4861(2021)07-1277-07
DOI: 10.11862/CJIC.2021.151

Synthesis, Crystal Structure and Cytotoxicity of Ru(Ⅱ) Complex Targeting DNA

GAI Shuang-Shuang[1] LAN Jun-Feng[2] ZHANG Peng[1,2] JIANG Cai-Yun*[,1,2] QIN Yi-Ming*[,1,2]
([1]*Key Laboratory for Research and Development of Characteristic Yao, Guangxi Science & Technology Normal University, Laibin, Guangxi* 545004, *China*)
([2]*School of Food and Biochemical Engineering, Guangxi Science & Technology Normal University, Laibin, Guangxi* 545004, *China*)

Abstract: To develop a novel antitumor Ru agent, [Ru(L)(DMSO)$_2$Cl$_2$] (**1**) (DMSO=dimethyl sulfoxide) was synthesized by employing a Schiff base ligand 3-methyl-2-thiophenecarboxaldehyde-4-hydroxybenzhydrazide (L). The single crystal X-ray crystallographic study was carried out to determine the crystallographic structure of **1**. The structure of complex **1** is composed of a central Ru(Ⅱ) ion, two DMSO molecules, two chloride ions, and a ligand L. In addition, **1** possessed strong antitumor activity against T24 cells by MTT analysis. Furthermore, the potential antitumor mechanism of **1** was investigated by comet assays, western-blotting assays, and DNA agarose gel electrophoresis. These results indicate that **1** can effectively bind to DNA and induce DNA damage, and eventually kill the tumor cells. DNA damage may be caused by the production of reactive oxygen species. CCDC: 2080249.

Keywords: ruthenium(Ⅱ) complex; DNA target; T24 cells; anticancer activity

Cancer seriously endangers people′s life and safety. In 2018, the World Health Organization reported that cancer was the second leading cause of death, killing about 9.6 million people worldwide[1]. Chemotherapy is a major method widely applied in current clinical cancer treatment[2-3]. Cisplatin is one of the most effective chemotherapeutic drugs approved by the Food and Drug Administration[4]. However, cisplatin is limited in clinical use due to its severe side effects[5-7]. Therefore, a range of metal complexes have been designed and

收稿日期:2020-12-15。收修改稿日期:2021-04-29。
广西高校中青年教师科研基础能力提升项目(No.2019KY0853,2020KY23016)资助。
*通信联系人。E-mail:jiangcaiyun2013@163.com,qym68@163.com

synthesized for the treatment of cancer[8-11], of which ruthenium complexes are the most promising to be the next generation of anticancer agents[12-13].

Many Ru complexes, such as KP-1019 and NAMI-A, have been widely studied due to their excellent clinical efficacy[14-15]. Ru complexes have been applied in various fields of medicinal chemistry against tumors with different biological targets[16-17]. In addition, aroylhydrazones possess excellent biological and pharmaceutical activities, including anticancer, anti-inflammatory, and anti-tubercular activities[18]. More importantly, previous studies have been showed that anticancer activity of metal-base complexes derived from aroylhydrazones were higher than that of the ligands alone[19-20]. Hence, the design of aroylhydrazone complexes chelated with ruthenium ion for anticancer treatment has an important prospect.

The primary target of metal-based agents to kill tumors is DNA, which causes amount of DNA lesions, thus preventing transcription and replication[21-22]. Considering the above factors, we designed and synthesized a Ru(Ⅲ) complex derived from aroylhydrazones (Scheme 1). Subsequently, the structure of Ru(Ⅲ) complex was measured via X-ray crystallography and solved. Finally, the anticancer activity of Ru(Ⅲ) complex and its effect on DNA were investigated *in vitro*.

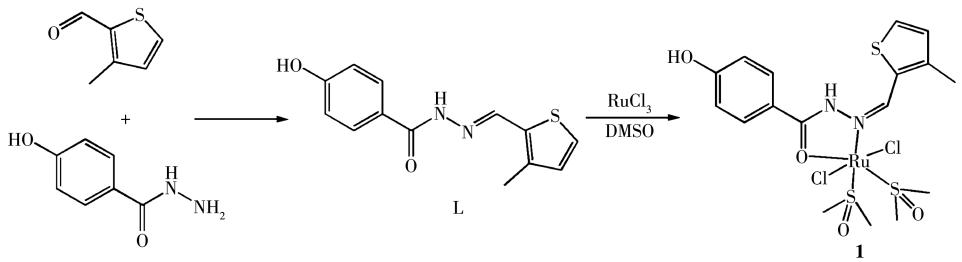

Scheme 1 Synthetic route for $[Ru(L)(DMSO)_2Cl_2]$ (**1**)

1 Experimental

1.1 Materials and general methods

The chemical reagents and solvent used were analytically pure and purchased from Sigma or Innochem Company. Tumor cell lines were supplied by the Shanghai institute for biochemistry and cell biology.

1.2 Synthesis of $[Ru(L)(DMSO)_2Cl_2]$ (1)

A mixture of 0.1 mmol 4-hydroxybenzhydrazide and 0.1 mmol 3-methyl-2-thiophenecarboxaldehyde were dissolved in 20 mL methanol and refluxed. Then the ligand L was obtained. Subsequently, 0.1 mmol $RuCl_3$ and 50 μL DMSO (dimethyl sulfoxide) were added and stirred for another 2 h (Scheme 1). The resulting solution was evaporated at room temperature, and the yellow-brown crystals crystallized after about 7 d. The purity of complex **1** (>95%) was detected by HPLC (Fig. S1). Anal. Calcd. for $C_{17}H_{26}Cl_2N_2O_5RuS_3$(%): C, 33.66; H, 4.32; N, 4.62. Found(%): C, 33.72; H, 4.35; N, 4.58.

1.3 X-ray crystallography

A single crystal (0.18 mm×0.19 mm×0.22 mm) of **1** was picked out and then measured by a Bruker SMART Apex Ⅱ CCD diffractometer with graphite-monochromated Mo *Kα* radiation (λ =0.071 073 nm). The diffraction data were collected. The structure was solved by direct methods and refined with the XL refinement package using least squares minimization by olex 2.0 software[23]. All non-hydrogen atoms were anisotropically refined. All hydrogen atoms were fixed in calculated positions and refined isotropically. The data is listed in Table 1, and selected bond lengths and angles are listed in Table 2.

CCDC: 2080249.

1.4 MTT assays

The human balder cell lines T24 were cultured in 96-well plate and incubated with the selected concentrations of complex **1** for 48 h. Then the MTT (3-(4,5-dimethylthiazol-2-yl)-2,5-diphenyltetrazolium bromide) solution was added to each well and incubated for 4 h. The medium was replaced with 100 μL DMSO. The absorbance was measured at an excitation wavelength of 570 or 630 nm with an enzyme-labelling instrument.

Table 1　Crystal data and structure refinement for complex 1

Empirical formula	$C_{17}H_{24}Cl_2N_2O_4RuS_3 \cdot H_2O$	D_c / (g·cm^{-3})	1.673
Formula weight	606.55	μ / mm^{-1}	1.163
Crystal system	Orthorhombic	F(000)	2 464
Space group	*Pbca*	Reflection collected	12 030
a / nm	1.702 43(6)	Independent reflection	4 241 (R_{int}=0.033 8, R_σ=0.042 4)
b / nm	1.595 86(7)	Data, restraint, parameter	4 241, 0, 276
c / nm	1.773 00(15)	Goodness-of-fit on F^2	1.149
Volume / nm^3	4.817 0(5)	Final R indexes [$I \geqslant 2\sigma(I)$]	R_1=0.065 7, wR_2=0.139 7
Z	8	Final R indexes (all data)	R_1=0.098 5, wR_2=0.163 4

Table 2　Selected bond lengths (nm) and angles (°) of complex 1

Ru1—S1	0.223 1(3)	Ru1—Cl2	0.238 4(3)	Ru1—N1	0.209 2(8)
Ru1—Cl1	0.240 0(3)	Ru1—O1	0.209 3(7)	Ru1—S2	0.225 2(3)
S1—Ru1—Cl1	91.87(12)	O1—Ru1—Cl1	88.4(2)	N1—Ru1—Cl2	84.8(3)
S1—Ru1—Cl2	92.49(13)	O1—Ru1—Cl2	86.7(2)	N1—Ru1—O1	77.6(3)
S1—Ru1—S2	93.21(10)	O1—Ru1—S2	90.9(2)	N1—Ru1—S2	168.5(2)
Cl2—Ru1—Cl1	171.35(12)	N1—Ru1—S1	98.2(2)	S2—Ru1—Cl1	93.46(10)
O1—Ru1—S1	175.8(2)	N1—Ru1—Cl1	87.2(3)	S2—Ru1—Cl2	93.75(12)

1.5　DNA cleavage studies

The super-coiled plasmid pBR322 DNA was incubated with complex **1** for 4 h. Subsequently, agarose gel electrophoresis was employed to isolate pBR322 DNA in the reaction solution. These results were captured by camera for analyzing the ability of complex **1** to cleave DNA.

1.6　Western-blotting

T24 cells were co-incubated with Ru(Ⅱ) complex for 24 h, and then the cells were harvested and lysed to obtain the proteins. The concentrations of proteins were measured using BCA assay. The proteins were isolated by SDS-polyacrylamide gel, transferred to a PVDF (polyvinylidene fluoride) membrane and blocked with fat-free milk. Then, the membrane was incubated with primary antibodies and secondary antibodies respectively.

1.7　DNA metalation

Two millions T24 cells were placed into 10 cm dishes, and incubated with complex **1** for 24 h. T24 cells were collected by centrifugation and washed once time. Subsequently, DNA was extracted using a PureLink Genomic DNA Mini Kit (Invitrogen). DNA purity was detected by absorbance measurements at 260 and 280 nm. The DNA solution was added 1 mL of concentrated HNO_3 and 0.5 mL of 30% H_2O_2. Finally, these samples were detected by ICP-MS.

1.8　Cellular uptake

T24 cells were seeded into 10 cm dishes, and then incubated with complex **1**. After 24 h, the cells were collected and washed. Subsequently, the cellular components were isolated and extracted according to the instructions of the mitochondrial isolation kit and the nuclear isolation kit, respectively. The samples were detected by ICP-MS.

1.9　Docking

The binding mode of complex **1** in DNA (PDB ID: 1D64) was investigated using AutoDock 4.0. Target receptor (DNA) and complex **1** were prepared via docking protocol and saved into 'PDBQT' format. And then the 'autogrid' and 'autodock' were performed, respectively. Energy-scoring function was used to ensure the best Ru(Ⅱ) complex-DNA pose.

1.10　Intracellular reactive oxygen species (ROS) analysis

T24 cells were cultured into 6-well plates, and treated with complex **1** for 24 h. After incubation, T24 cells were collected and stained in the dark with 2′,7′-

dichlorodihydro-fluorescein diacetate (H_2DCF-DA) for 30 min. Intracellular ROS generation was detected by flow cytometry.

1.11 Comet assay

T24 cells were incubated with complex **1** for 24 h, and the cells were harvested. 1×10^4 cells were embedded in 80 μL low-gelling-temperature agarose and rapidly pipetted onto a pre-coated microscope slide. These slides were electrophoresed for 20 min, and then stained with PI for 30 min in dark. Finally, the slides were graphed using a laser confocal microscope.

2 Results and discussion

2.1 Structure of 1

X-ray diffraction analysis reveals that **1** crystallizes in the orthorhombic space group *Pbca*. As shown in Fig. 1, the structure of complex **1** is composed of a central Ru(Ⅲ) ion, two DMSO molecules, two chloride ions, and a Schiff base ligand L. The central Ru(Ⅲ) forms a six-coordinated environment, which is composed of one N atom (Ru1—N1 0.209 2 nm) and one O atom (Ru1—O1 0.209 3 nm) of HL, two S atoms (Ru1—S1 0.223 1 nm, Ru1—S2 0.225 2 nm) of DMSO and two Cl atoms (Ru1—Cl1 0.240 0 nm, Ru1—Cl2 0.238 4 nm).

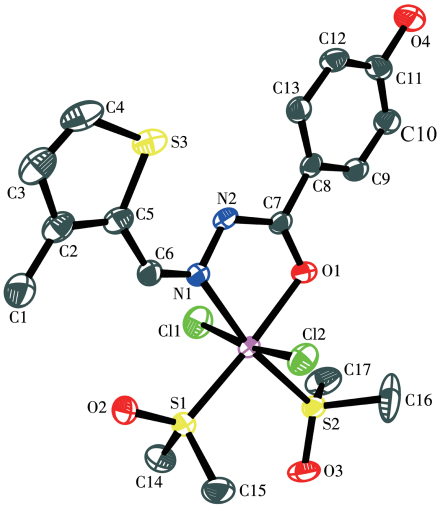

One crystalline water molecule is not shown

Fig.1 ORTEP diagram of complex **1** showing 30% probability level ellipsoids

2.2 Anticancer activity of 1

The cytotoxicity of **1** against T24 cells was assessed using the MTT assay. The IC_{50} values of HL, $RuCl_3$ and DMSO were greater than 50 μmol·L^{-1}. These results indicate that the compounds do not exhibit significant antitumor activity. While the synthesized complex **1** from the ligand and $RuCl_3$ exhibited remarkably activity (IC_{50}=15.28 μmol·L^{-1}), as shown in Fig.2.

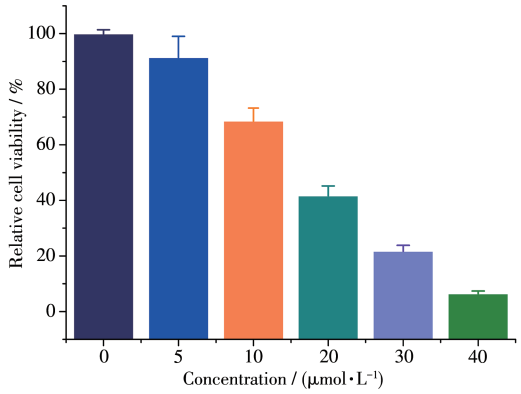

Fig.2 Cytotoxicity of **1** at different concentrations

2.3 Cellular accumulation

The cellular uptake of **1** by T24 cells was measured using ICP-MS. As shown in Fig.3, the contents of ruthenium in cells, nuclei and mitochondria after treatment of **1** were 1.23, 0.28 and 0.11 nmol, respectively. These results suggest that **1** can efficiently enter the cell and accumulate in the nucleus.

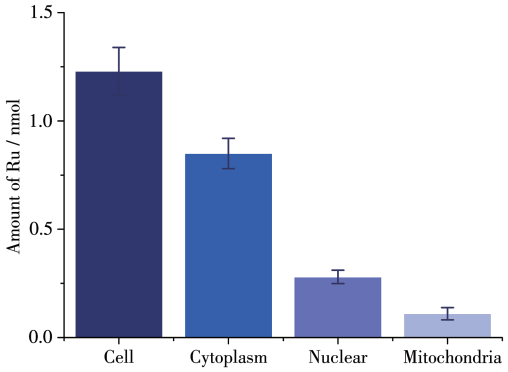

Fig.3 ICP-MS analysis of total Ru contents in cytoplasm, mitochondria, and in nucleus of T24 cells (1×10^6 cells) treated with **1** for 24 h

2.4 Anti-tumour mechanism of 1

2.4.1 DNA cleavage

DNA is the primary intracellular target of many PT/Ru drugs in the treatment of tumors[21-22]. Hence, the DNA-cleaving activity of **1** was investigated by an agarose gel electrophoresis assay using pBR322 DNA. The

control group cannot cleave the PBR322 DNA, whereas **1** can efficiently relax the supercoiled form (Form Ⅰ) of pBR322 DNA into open circular form (Form Ⅱ) in a dose-dependent manner. These results strongly suggest that complex **1** has a strong effect on DNA (Fig.4).

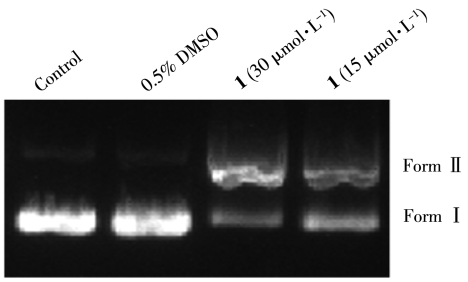

Fig.4　Agarose gel electrophoresis patterns for cleavage of pBR322 DNA by **1**

2.4.2　Docking studies

To better understand the mode between B-DNA and **1**, molecular docking was carried out for studying the interactions. Complex **1** fitted well into the curved profile of the B-DNA in the minor groove located in the A-T rich region (Fig.5). The energy minimization structure indicates that **1** is stabilized by hydrophobic contact, van der Waals forces and B-DNA functional groups.

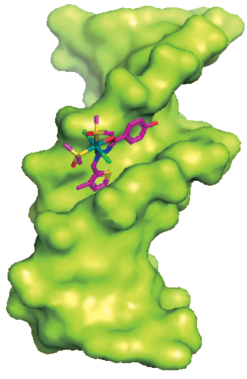

Fig.5　Molecular docked model of **1** with B-DNA

2.4.3　DNA damage studies

To further confirm the ability of **1** acting on DNA in tumor cells, the genomic DNA was extracted from T24 cells after treated with **1**. The Ru content in the genomic DNA was at highly level, and the significantly elevated level of Ru content was in a dose-dependent fashion (Fig.6).

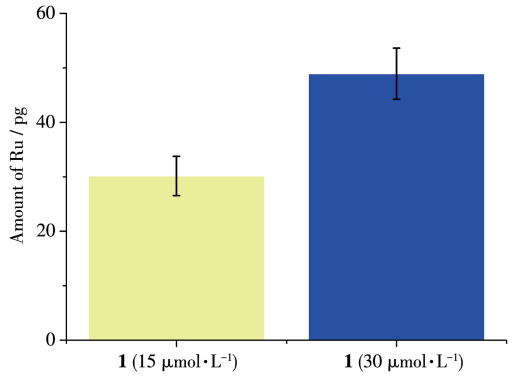

Fig.6　Amount of Ru in genomic DNA (1 μg) of T24 cells after treatment of **1**

T24 cells were induced apparent DNA damage co-incubated with complex **1**, which was characterized by the tail DNA. The number and length of tail DNA were in positive correlation with the degree of DNA damage. The **1**-treated group produced more and longer tail DNA in a dose-dependent manner than the control group (Fig.7).

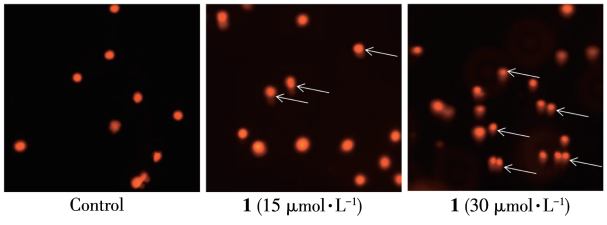

Tail DNA was marked with white arrow

Fig.7　Comet assay for analyzing DNA damage of T24 cells after treatment of **1**

Western blotting assays showed that the expression level of γH2AX (a well-known marker for DNA double-strand breaks) in the control group was kept at lower levels, while that in the treatment group significantly increased (Fig.8). Taken together, these results strongly indicate that direct interaction with DNA is a possible mechanism for complex **1** to play a role in kill-

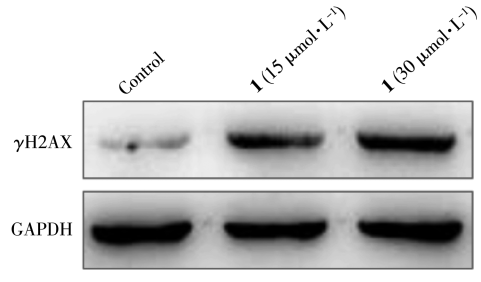

Fig.8　Expression level of γH2AX treated with **1**

ing tumor cells.

2.4.4 ROS generation

Generally, ROS is, at least in part, responsible for the cleavage of DNA[24-26]. Therefore, the amount of intracellular ROS after treatment of **1** was investigated by flow cytometry using the DCFH-DA. T24 cells treated with **1** led to a shift in the fluorescence peak to the right compared to the un-treatment group, which indicate that **1** significantly increases intracellular ROS levels in a dose-dependent fashion (Fig.9).

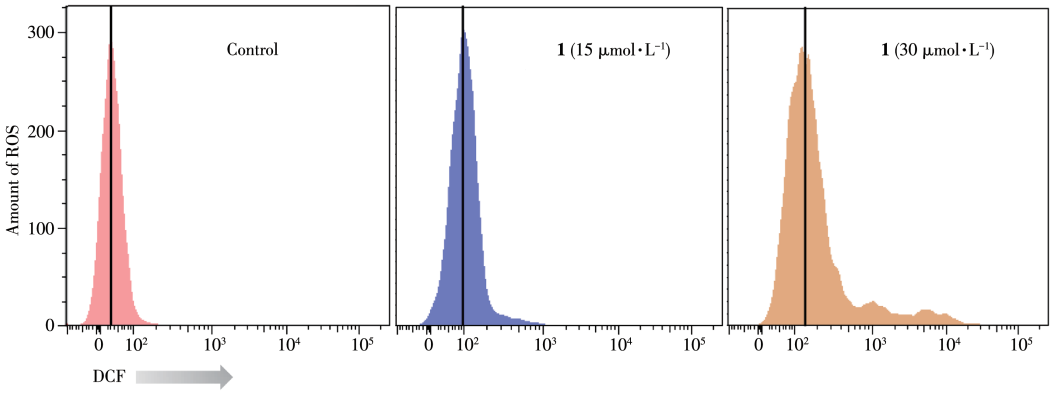

Fig.9 Analysis of ROS levels in T24 cells treated with **1** for 24 h

3 Conclusions

A Ru(Ⅱ) complex, $[Ru(L)(DMSO)_2Cl_2]$ (**1**), was synthesized and its anticancer activity was investigated. Complex **1** exhibited effective activities against T24 cells, whereas the ligands had no significant cytotoxicity. Complex **1** is possible to kill tumor cells through the following mechanisms: **1** can bind to DNA bases, form DNA adducts, induce genomic DNA damage, and may block transcription and replication. Additionally, **1** can produce amount of ROS, causing oxidative loss of T24 cells, which leads to tumor cell death. In summary, complex **1** has potential as an anti-cancer chemotherapeutic agent. Our studies may be useful in guiding the development for designing new metal-base antitumor agents.

Supporting information is available at http://www.wjhxxb.cn

References:

[1] El-Kordy E A. *J. Microsc. Ultrastruct.*, **2019**,**7**:153-164

[2] Mukaya E H, Mbianda X Y. *Mini-Rev. Med. Chem.*, **2020**,**20**:726-738

[3] Schweigert M, Dubecz A, Stein H J. *Nat. Rev. Gastroenterol. Hepatol.*, **2013**,**10**:230-244

[4] Rancoule C, Guy J B, Vallard A, Ben Mrad M, Rehailia A, Magné N. *Bull. Cancer*, **2017**,**104**:167-176

[5] Rosenberg B, Van Camp L, Krigas T I. *Nature*, **1965**,**205**:698-699

[6] Rosenberg B, Van Camp L, Grimley E B, Thomson A J. *J. Biol. Chem.*, **1967**,**242**:1347-1352

[7] Notaro A, Frei A, Rubbiani R, Jakubaszek M, Basu U, Koch S, Mari C, Dotou M, Blacque O, Gouyon J, Bedioui F, Rotthowe N, Winter R F, Goud B, Ferrari S, Tharaud M, Řezáčová M, Humajová J, Tomšík P, Gasser G. *J. Med. Chem.*, **2020**,**63**:5568-5584

[8] Misirlic-Dencic S, Poljarevic J, Isakovic A M, Sabo T, Markovic I, Trajkovic V. *Curr. Med. Chem.*, **2020**,**27**:380-410

[9] Sun Y, Heidary D K, Zhang Z, Richards C I, Glazer E C. *Mol. Pharm.*, **2018**,**15**:3404-3416

[10] Mudavath R, Vuradi R K, Bathini U, Narsimha N, Kunche S, Sunitha S N T, Ch S D. *Nucleosides Nucleotides Nucleic Acids*, **2019**, **38**:874-900

[11] Leskovac A, Petrovic S, Lazarevic-Pasti T, Krstic M, Vasic V. *J. Biol. Inorg. Chem.*, **2018**,**23**:689-704

[12] Biancalana L, Pampaloni G, Marchetti F. *Chimia (Aarau)*, **2017**,**71**: 573-579

[13] Alessio E, Messori L. *Molecules*, **2019**,**24**:1995-2014

[14] Trondl R, Heffeter P, Kowol C R, Jakupec M A, Berger W, Keppler B K. *Chem. Sci.*, **2014**,**5**:2925-2932

[15] Nardon C, Brustolin L, Fregona D. *Future Med. Chem.*, **2016**,**8**:211-226

[16] Notaro A, Gasser G. *Chem. Soc. Rev.*, **2017**,**46**:7317-7337

[17] Hartinger C G, Jakupec M A, Zorbas-Seifried S, Groessl M, Egger A, Berger W, Zorbas H, Dyson P J, Keppler B K. *Chem. Biodivers.*, **2008**,**5**:2140-2155

[18] Samanta B, Chakraborty J, Shit S, Batten S R, Jensen P, Masuda J D, Mitra S. *Inorg. Chim. Acta*, **2007**,**360**:2471-2484

[19] Deng J G, Gou Y, Chen W. Fu X, Deng H. *Bioorg. Med. Chem.*, **2016**,**24**:2190-2198

[20] Monfared H H, Vahedpour M, Yeganeh M M, Ghorbanloo M, Mayer

P, Janiak C. *Dalton. Trans.*, **2011**,**40**:1286-1294

[21]Rocha C R, Silva M M, Quinet A, Cabral-Neto J B, Menck C. *Clinics* (*Sao Paulo*), **2018**,**73**:478-488

[22]Rodríguez-Corrales J Á, Wang J, Winkel B S J, Brewer K J. *ChemBioChem*, **2018**,**19**:2216-2224

[23]Dolomanov O V, Bourhis L J, Gildea R J, Howard J A K, Puschmann H. *J. Appl. Crystallogr.*, **2009**,**42**:339-341

[24]Celik H, Arinç E. *J. Pharm. Pharm. Sci.*, **2008**,**11**:68-82

[25]Pracharova J, Radosova M T, Dvorak T E, Thangappan R, Arivanandhan M. *Dalton. Trans.*, **2016**,**45**:13179-13186

[26]Wani T H, Chakrabarty A, Shibata N, Yamazaki H, Guengerich F P, Chowdhury G. *Chem. Res. Toxicol.*, **2017**,**30**:1622-1628